IEEE Access
Multidisciplinary ⋮ Rapid Review ⋮ Open Access Journal

Received 1 June 2022, accepted 16 June 2022, date of publication 24 June 2022, date of current version 30 June 2022.

Digital Object Identifier 10.1109/ACCESS.2022.3186093

Rank-Sum-Weight Method Based Systematic Determination of Weights for Controller Tuning for Automatic Generation Control

P. J. KRISHNA[1], (Member, IEEE), V. P. MEENA[1], (Member, IEEE), V. P. SINGH[1], (Senior Member, IEEE), AND BASEEM KHAN[2], (Senior Member, IEEE)

[1]Department of Electrical Engineering, Malaviya National Institute of Technology Jaipur, Jaipur 302017, India
[2]Department of Electrical and Computer Engineering, Hawassa University, Hawassa 05, Ethiopia

Corresponding author: Baseem Khan (baseem.khan04@gmail.com)

ABSTRACT The design and performance evaluation of a grey wolf optimizer (GWO) aided rank-sum-weight method based proportional-integral-derivative regulator with derivative filter for automatic generation control of two-area interconnected power systems are presented in this research. The derivative gain filter is used to lessen the impacts of noise in the input signal. Sub-objectives based on integral of time multiplied square error (ITSE) of frequency deviations, tie-line power deviation, and area-control errors (ACEs) are used to formulate the objective function for adjusting regulator settings. A single overall objective function is formed by combining these sub-objectives. ITSEs of two areas, ITSEs of tie-line power deviation, and ITSEs of ACEs of two areas comprise up the overall objective function. In the control design, the weights in the overall objective function are used to evaluate relative significance of each sub-objective. In contrast to previous techniques, where weights are either considered equal by ignoring the relative relevance of sub-objectives or selected randomly, the weights in this article are obtained using the rank-sum-weight method systematically. Using the GWO algorithm, the overall objective function is minimized. For six different circumstances including different load disturbances in interconnected areas, the effectiveness of the proposed GWO aided rank-sum-weight method based controller is examined. The performance of the GWO-tuned controller is also compared to those of other controllers tuned using the differential evolution, elephant herding optimization, Nelder-Mead simplex, membrane computing, and Luus-Jaakola algorithms. Time domain specifications are tabulated for each of the six circumstances. The findings are also plotted to demonstrate the frequency and tie line power fluctuations. A statistical analysis is also performed in order to assess the overall efficacy of the suggested controller.

INDEX TERMS Automatic generation control, Grey wolf optimization, proportional-integral-differential controller, rank-sum-weight method.

I. INTRODUCTION

Whenever there is a change in either system frequency or tie-line loading, or a combination of both, the regulation of output electrical power from electric generators in a specific region is defined as the automatic generation control (AGC). Electric power is exchanged across the areas within established boundaries in order to sustain scheduled system frequency. Because of the following factors, AGC [1], [2] is required:

1) For generating enough electricity to fulfil all load needs.
2) To keep the interconnected power system's frequency at nominal operating level.
3) As soon as feasible, to reduce the deviation of tie-line power from preset interchanges among control areas.
4) To achieve optimal generation scheduling.

Studies on AGC of single-area power systems [3]–[5], two-area power systems [6]–[8], three-area power systems [9]–[11], and multi-area power systems [12]–[14] have been published. It is also obvious from the literature that various contributions mention mostly linear models of power systems in the form of transfer functions. The proportional-integral-derivative (PID) controllers are primarily developed to regulate the overall

The associate editor coordinating the review of this manuscript and approving it for publication was Zhenzhou Tang.

system [4], [5], [12], [15]–[20], since transfer functions are used to describe the power systems investigated. Other kind of PID controllers include proportional-integral (PI) [21], integral-double derivative (IDD) [22], proportional-integral-double derivative (PIDD) [23], proportional-derivative cascaded proportional-integral (PD-PI) [24], and cascaded PI-PD [25], cascaded PID-PID [26] controllers.

To ensure tie-line power exchange and frequency of interconnected power system within predefined bounds, controller parameters must be tuned for optimal and reliable power flow. PID tuning methods are divided into three categories depending on the tuning process:

1) Manual tuning,
2) Rule-based tuning, and
3) Meta-heuristic based tuning.

Meta-heuristic based tuning has recently been adopted to tune controllers, since it delivers superior performance characteristics than manual and rule-based tuning approaches. Optimization techniques utilized are meta-heuristic approaches to minimise the objective function specified for controller tuning. Genetic algorithm [27], [28], gravitational search algorithm [29], [30], bacteria foraging optimization [31], [32], bat algorithm [33], [34], teaching learning based optimization [35], [36], firefly algorithm [37], [38], particle swarm optimization [39], [40], artificial bee colony [41], [42], jaya algorithm [19], [43], and whale optimization [15], [44] are some of the algorithms used in literature for tuning PID controllers for AGC.

Performance indices such as integral of absolute error (IAE) [28], [39], an integral of squared error (ISE) [32], [44], an integral of time multiplied absolute error (ITAE) [45], [46], an integral of time multiplied square error (ITSE) [45], [46] are used to formulate objective functions for tuning controller settings. Frequency deviations, tie-line power variations, and area control errors (ACEs) of interconnected areas are all examined using these performance indicators. The researchers in [27] examined ISE, in order to attain controller parameters for a two-area interconnected power system. According to the findings of this research, individual ISE of ACEs from two areas are combined to form the overall objective function. In [31], the use of ISE to get controller parameters for a three-area linked power system is examined. As per the results of this study, individual ISE of ACEs from the three areas under consideration are combined to produce the overall objective function. The researchers in [32] also procured ISE to perform controller parameter tuning. The findings from this study indicate that individual ACEs from both areas of the power system are used to obtain a overall objective function.

In [11], to achieve controller parameters of a three-area interconnected power system, ISEs of frequency deviation in area-1 and area-2, as well as tie-line power deviation, are evaluated. These ISEs of frequency variations, as well as tie-line power deviation in a three-area interconnected power system, are combined to produce the overall objective function. The researchers in [12] considered ITAE to acquire controller parameters for a five-area interconnected power system. For the purpose of formulating the objective function, the ACEs of a five-area interconnected system are taken into account. In [28], for the formulation of the objective function, more than one performance indices are considered. The objective function is formulated using a combination of ISE, ITAE, ITSE, integral of squared time multiplied absolute error (ISTAE) and integral of squared time multiplied squared error (ISTSE) of frequency deviations of area-1 and area-2, as well as tie-line power. These performance metrics, evaluated in the objective function, are either incorporated directly without considering relative relevance or are given equal weights in the literature [17], [27], [31], [32], [34], [42], [47], [48]. To construct a better objective function for controller realization, a systematic process should be used to determine relative weights of distinct performance criteria.

In this article, a PID regulator for AGC of a two-area linked power system is constructed utilising the grey wolf optimization algorithm assisted with a systematic technique namely rank-sum-weight method. ITAEs of deviation in frequencies of area-1 and area-2, ITAEs of deviation in tie-line power of interconnected areas, and ITAEs of ACEs of area-1 and area-2 are used to formulate the objective function. These performance indices (i.e. ITAEs) are sub-objective functions that together constitute the overall objective function. The weighted summation of all these five ITAEs form the overall objective function. Weights associated with multiple sub-objective functions are usually chosen arbitrarily or given equal value in literature [17], [48], ignoring their relative significance. The significant contributions of this work include:

- The weights of the sub-objective functions examined in this study are derived systematically using rank-sum-weight method [49]. The weight calculations in rank-sum-weight method are based on relative relevance among the sub-objectives evaluated.
- The grey wolf optimization (GWO) algorithm is used to tune the PID controller parameters to maintain frequency deviation, tie-line power deviation, and ACEs within preset limits by minimising the overall objective function.
- To prove the efficacy and effectiveness of proposed GWO-based PID controller, other controllers tuned utilising differential evolution (DE), elephant herding optimization (DE), Nelder-Mead simplex (NMS), membrane computing (MC), and Luus-Jaakola (LJ) algorithms are compared.
- Furthermore, six distinct test circumstances are explored for evaluating the proposed GWO-PID controller's performance. The statistical analysis provided aids the effectiveness and efficacy of the suggested GWO-PID controller.

The following is a breakdown of this contribution. Section II describes the power system architecture that has been examined. The controller structure is also provided in Section II. In Section III, the problem formulation is provided. Section IV explains the rank-sum-weight method and

how it is used to AGC. In Section V, the grey wolf optimization algorithm is explained. In Section VI, the performance of the proposed controller is evaluated for six different test circumstances. Finally, in Section VII, the conclusion is stated, followed by future scope.

II. STUDIED POWER SYSTEM ARCHITECTURE

A power system is made up of a network of transmission lines that interconnect a large number of generators. Electrical power is delivered to consumers at rated voltage and frequency via these transmission lines. There are several energy sources for generating electrical power which include fossil fuels like natural gas, oil, and coal; and hydro, wind, solar, geothermal, nuclear, tidal, wave, biomass, etc. The energy gained from these sources is first transformed into mechanical energy. This mechanical energy is then converted to electrical energy with the help of generators. There are two types of power systems based on the number of generation and distribution networks:

1) Single-area power systems and
2) Multi-area power systems.

The increased load demand in a single-area power system is fulfilled either by borrowing rotating kinetic energy from machines in the power system or increasing generation whereas the increased load demand in a multi-area power system is fulfilled by power interchanges across interconnected areas through tie-lines.

A. CONFIGURATION OF MODEL UNDER INVESTIGATION

The Fig. 1 depicts the two-area power system investigated in this work. The examined two-area power system is considered from Ali and Abd-Elazim [50] along with the system parameters. It is a veristic linked system made up of two non-reheat thermal power plants with a total capacity of 2000 MW and a nominal load of 1000 MW each. A network of two-area power system is depicted in the Fig. 1 where Δf_{a1}, and Δf_{a2} are variations in system frequencies, ACE_{a1}, and ACE_{a2} are area control errors, μ_{a1}, and μ_{a2} are control inputs, β_{a1}, and β_{a2} are frequency bias factors, R_{a1}, and R_{a2} are governor speed regulation constants, τ_{gr1}, and τ_{gr2} are governor time constants, τ_{te1}, and τ_{te2} are turbine time constants, τ_{a1}, and τ_{a2} are power system time constants, κ_{a1}, and κ_{a2} are power system gains, ΔP_{gr1}, and ΔP_{gr2} are power deviations of governors, ΔP_{te1}, and ΔP_{te2} are power deviations of non-reheat steam turbines, ΔP_{la1}, and ΔP_{la2} are change in load demands of power system in area-1, and area-2 respectively. ΔP_{tl} is the change in tie-line power of interconnected power system.

B. CONFIGURATION OF CONTROLLER

As it is simple to comprehend and implement, PID controller is the most widely used feedback control mechanism. The controller structure used in this research is depicted in Fig. 2.

κ_{pg}, κ_{ig}, and κ_{dg} are three controller parameters in the controller structure which indicate proportional gain, integral gain, and derivative gain, respectively. These parameters must be tuned finely to fit the dynamics of the process under control. A filter η with derivative gain is used to reduce noise in the signal. The PID controller transfer function [50] with filter in derivative gain is given by

$$TF_{PIDn} = \kappa_{pg} + \kappa_{ig}\left(\frac{1}{s}\right) + \kappa_{dg}\left(\frac{1}{\frac{1}{\eta} + \frac{1}{s}}\right) \tag{1}$$

The area control errors, ACE_{a1} and ACE_{a2} of area-1 and area-2, respectively, are the controllers' inputs. The area control errors (ACEs) of area-1 and area-2 [50] are calculated as follows:

$$ACE_{a1}(s) = \Delta P_{tl12}(s) + \beta_{a1} \cdot \Delta F_{a1}(s) \tag{2}$$

$$ACE_{a2}(s) = a_{12} \cdot \Delta P_{tl12}(s) + \beta_{a2} \cdot \Delta F_{a2}(s) \tag{3}$$

III. PROBLEM FORMULATION

The aim of automatic generation control is to optimize the reliable and persistent power flow in a multi-area interconnected power system such that frequency fluctuations are reduced while the system's constraints are met. The formulation of an objective function is critical for finding the best solution to this problem. The tuning of a controller is based on well-defined objectives that meet the demands and limits of the system. The objective function as well as the various constraints are listed below.

A. OBJECTIVE FUNCTION FORMULATION

The effectiveness of an optimization is considerably influenced by the objective function selected. An integral error (IE), an integral of absolute error (IAE), an integral of squared error (ISE), an integral of time multiplied absolute error (ITAE) or an integral of time multiplied square error (ITSE) may be chosen for formulation of objective function. While tuning controller parameters, ITAE error minimization of frequency deviations, tie-line power deviation, and area control errors (ACEs) are among the design objectives covered in this article. The following are the various minimization objectives considered.

$$\Gamma_1 = \int_0^{\tau_s} |\Delta f_{a1}| t \, dt + \int_0^{\tau_s} |\Delta f_{a2}| t \, dt \tag{4}$$

$$\Gamma_2 = \int_0^{\tau_s} |\Delta P_{tl}| t \, dt \tag{5}$$

$$\Gamma_3 = \int_0^{\tau_s} |ACE_{a1}| t \, dt + \int_0^{\tau_s} |ACE_{a2}| t \, dt \tag{6}$$

where, τ_s denotes the overall simulation time. The first objective function, Γ_1 studied is a combination of ITAE of deviation in system frequencies of area-1 and area-2. The second objective function studied is Γ_2, which defines the ITAE of power deviation in tie-line. The third objective function studied is Γ_3, which describes the ITAE of deviation in ACEs

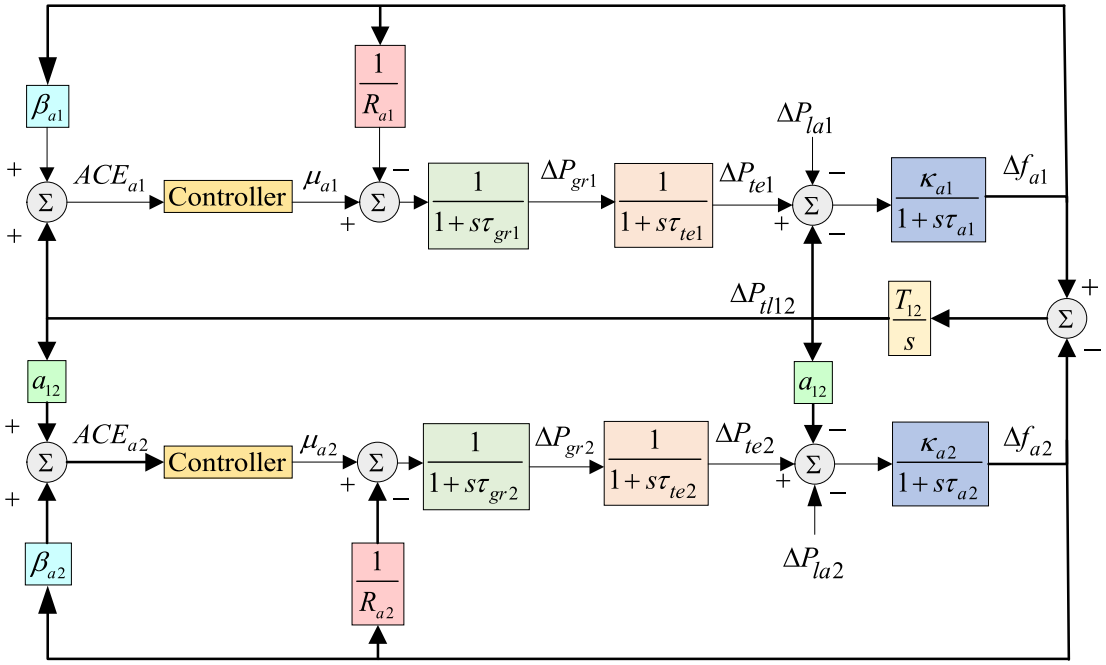

FIGURE 1. Block diagram of two-area power system.

of area-1 and area-2. The total objective function, taking into account all three objectives, is as follows:

$$\Gamma(\Gamma_1, \Gamma_2, \Gamma_3) = \varepsilon_1\Gamma_1 + \varepsilon_2\Gamma_2 + \varepsilon_3\Gamma_3 \tag{7}$$

where, the weights of the objectives Γ_1, Γ_2, and Γ_3 are ε_1, ε_2, and ε_3 respectively. These weights show the relative significance of the sub-objectives in the overall objective. Most of the time, the relative importance of objectives is overlooked or viewed as a set of arbitrary values. The overall aim established utilising the sub-objectives is deemed to be of similar relative importance, as indicated in literature [17], [48]. The overall objective function in (7) is realised by combining (4), (5), and (6) and can be formulated as follows.

$$\left.\begin{aligned}\Gamma = \varepsilon_1 &\left(\int_0^{\tau_s} |\Delta f_{a1}|t\ dt + \int_0^{\tau_s} |\Delta f_{a2}|t\ dt\right)\\ &+ \varepsilon_2 \int_0^{\tau_s} |\Delta P_{tl}|t\ dt\\ &+ \varepsilon_3 \left(\int_0^{\tau_s} |ACE_{a1}|t\ dt + \int_0^{\tau_s} |ACE_{a2}|t\ dt\right)\end{aligned}\right\} \tag{8}$$

In this article, the weights ε_1, ε_2, and ε_3 associated with (8) are determined in a methodical way. The individual weightage of each objective function Γ_1, Γ_2, and Γ_3 specified in (4), (5), and (6), respectively, appearing in the overall objective function, Γ, is obtained using rank-sum-weight method [49].

B. CONSTRAINTS

The overall objective function for this AGC problem is derived in (8). Controller parameters, κ_{pg}, κ_{ig}, κ_{dg}, and

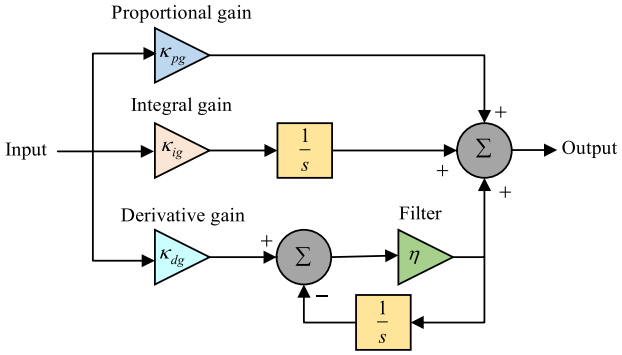

FIGURE 2. Block diagram of PID controller with derivative filter.

derivative filter coefficient, η, are among the decision factors, as illustrated in Fig. 2. The boundary conditions of the controller parameters taken into account are as follows

$$\kappa_{pg}^{min} < \kappa_{pg} < \kappa_{pg}^{max} \tag{9}$$
$$\kappa_{ig}^{min} < \kappa_{ig} < \kappa_{ig}^{max} \tag{10}$$
$$\kappa_{dg}^{min} < \kappa_{dg} < \kappa_{dg}^{max} \tag{11}$$
$$\eta^{min} < \eta < \eta^{max} \tag{12}$$

IV. RANK-SUM-WEIGHT METHOD AND ITS IMPLEMENTATION TO AGC

Rank-sum-weight method is a multi-attribute-decision-making methodology proposed by Stillwell *et al.* [49]. The rank-sum-weight method is used for weighing of attributes with respect to each other for decision making problem.

Firstly, attributes are identified. Then, the rank ordering of the attributes in the attribute set are decided. From this information, the weight [49] for the given attribute is determined by

$$\varepsilon_r = \frac{\chi - \vartheta_r + 1}{\sum_{r=1}^{\chi} (\chi - \vartheta_r + 1)} \tag{13}$$

where, χ denotes the total number of attributes, ϑ_r indicates the rank position of r^{th} attribute and ε_r gives the normalized weight of r^{th} attribute. In this contribution, three sub-objectives formulated are considered as attributes (i.e. $\chi = 3$). The attributes considered are Γ_1, Γ_2, and Γ_3 as given in (4), (5) and (6), respectively. Once, the attributes are considered, the rank ordering of these sub-objectives is accomplished as given in Table 1.

TABLE 1. Ranking order of sub-objectives.

Sub-objective	Rank (ϑ_r)
Γ_1	1
Γ_2	2
Γ_3	3

The ranking order of sub-objectives is considered as Γ_1, Γ_2 and Γ_3 in order. This ranking order of sub-objectives is considered because the effect of change in load will be very high on ITAE of deviations in frequencies of both the areas followed by ITAE of deviations in tie-line power and ITAE of ACEs of both the areas. Now, the normalized weight of each sub-objective is obtained from (13) as

$$\left.\begin{aligned} \varepsilon_1 &= 0.5\,; \\ \varepsilon_2 &= 0.3333\,; \\ \varepsilon_3 &= 0.1666 \end{aligned}\right\} \tag{14}$$

These weights depict the weighing factor of sub-objective in the overall objective function. Thus, the overall objective function (7) with Γ_1, Γ_2, and Γ_3 and their weights ε_1, ε_2, and ε_3 respectively, turns out to be

$$\left.\Gamma(\Gamma_1, \Gamma_2, \Gamma_3) = 0.5\,\Gamma_1 + \ 0.3333\,\Gamma_2 + \ 0.1666\,\Gamma_3\right\} \tag{15}$$

From (4), (5), and (6), the overall objective function obtained in (15) is rewritten as

$$\left.\begin{aligned} \Gamma = 0.5 &\left(\int_0^{\tau_s} |\Delta f_{a1}|t\ dt + \int_0^{\tau_s} |\Delta f_{a2}|t\ dt\right) \\ &+ 0.3333 \int_0^{\tau_s} |\Delta P_{tl}|t\ dt \\ &+ 0.1666 \left(\int_0^{\tau_s} |ACE_{a1}|t\ dt + \int_0^{\tau_s} |ACE_{a2}|t\ dt\right) \end{aligned}\right\} \tag{16}$$

In order to obtain controller gains, the weighted objective function, given in (16), must be minimized. In this article, grey wolf optimizer is used to minimize (16), subject to constraints specified in (9), (10), (11), and (12).

V. GREY WOLF OPTIMIZATION ALGORITHM

In 2014, Mirjalili *et al.* [51] presented the grey wolf optimization (GWO) algorithm. It is based on the behaviour of grey wolves when they are exploring and hunting for prey. Grey wolves are members of the canidae family and are scientifically known as canis lupus. They are predators who prefer to live in a group namely pack. The social dominance order among these grey wolves is rigid. Grey wolves' behaviour is characterised by social hierarchy, encircling prey, hunting, exploitation, and exploration. In dependance on these behavioural patterns, grey wolves are divided into four categories: ρ, σ, ν and υ. The first level is ρ, and the wolf at this level is in charge of making judgments. The pack is bound to the judgments made by ρ. Wolves of this rank do not have to be the strongest members of the pack, but they are the greatest in terms of pack management. In this level of pack, the wolves demonstrate that group discipline and structure are more essential than collective power. The second level is σ, where the wolves aid the ρ level in decision-making and other endeavours. In the absence of a ρ level, the pack is officiated by the σ level. Wolves at the σ level promote ρ's choice all over the pack, even while providing feedback to ρ level on the judgment and its execution. Scouts, sentinels, hunters, and caretakers make up the third level of the ranking system (i.e. ν). Scouts are responsible for being vigilant when watching the territory's borders and informing the pack if there is a threat while sentinels are responsible for the pack's safety. During the search for prey, hunters are responsible for assisting ρ and σ levels. The pack's lowest ranking is the υ level. The wolves at this υ level are the last to devour food and are subject to submission by higher ranked wolves.

The new position of wolves [51] is calculated mathematically by aggregating the locations of ρ, σ and ν wolves in the search space.

$$\overline{\Psi}_{Itr+1} = \frac{\overline{\Psi}_\rho + \overline{\Psi}_\sigma + \overline{\Psi}_\nu}{3} \tag{17}$$

where, $\overline{\Psi}_{Itr+1}$ represents new position of wolves in search space, $\overline{\Psi}_\rho$ denotes new position of first level wolves (ρ), $\overline{\Psi}_\sigma$ represents new position of second level wolves (σ) and $\overline{\Psi}_\nu$ denotes new position of third level wolves (ν). The new positions of these three levels of wolves are calculated as

$$\overline{\Psi}_\rho = \overline{\Psi}_{\rho,Itr} - \overline{\Upsilon}_1 \cdot \overline{\Lambda}_\rho \tag{18}$$
$$\overline{\Psi}_\sigma = \overline{\Psi}_{\sigma,Itr} - \overline{\Upsilon}_2 \cdot \overline{\Lambda}_\sigma \tag{19}$$
$$\overline{\Psi}_\nu = \overline{\Psi}_{\nu,Itr} - \overline{\Upsilon}_3 \cdot \overline{\Lambda}_\nu \tag{20}$$

where, $\overline{\Psi}_{\rho,Itr}$, $\overline{\Psi}_{\sigma,Itr}$ and $\overline{\Psi}_{\nu,Itr}$ represent current positions of ρ, σ and ν level wolves respectively; $\overline{\Lambda}_\rho$, $\overline{\Lambda}_\sigma$, $\overline{\Lambda}_\nu$ denote the encircling behaviour of different levels of wolves. The encircling behaviour is given as

$$\overline{\Lambda}_\rho = \left|\overline{T}_1 \cdot \overline{\Psi}_{\rho,Itr} - \overline{\Psi}\right| \tag{21}$$
$$\overline{\Lambda}_\sigma = \left|\overline{T}_2 \cdot \overline{\Psi}_{\sigma,Itr} - \overline{\Psi}\right| \tag{22}$$
$$\overline{\Lambda}_\nu = \left|\overline{T}_3 \cdot \overline{\Psi}_{\nu,Itr} - \overline{\Psi}\right| \tag{23}$$

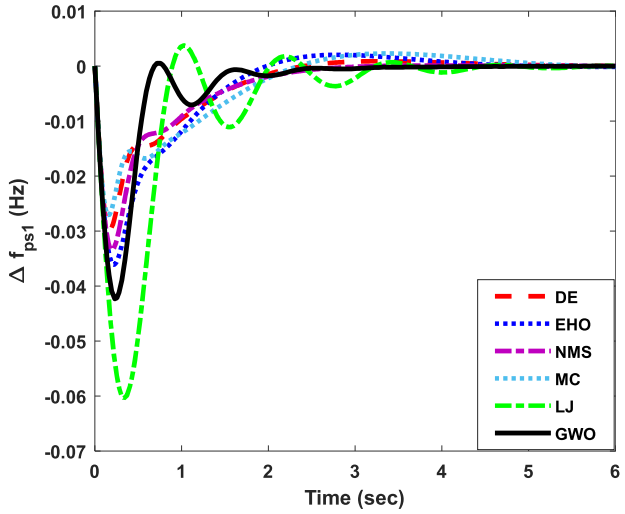

FIGURE 3. Frequency deviation of area-1 under Test Scenario 1.

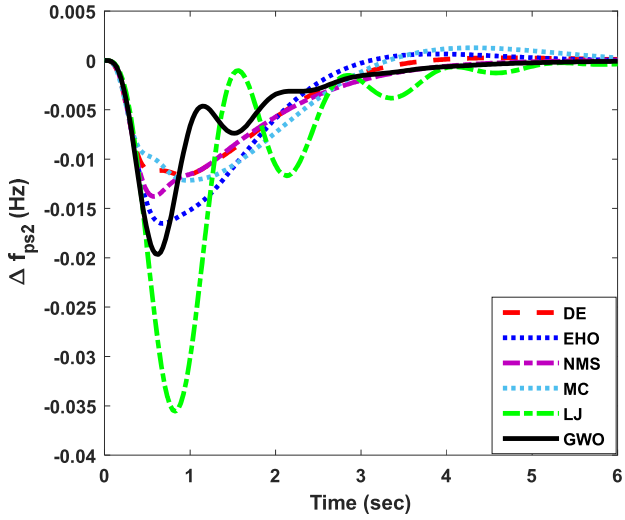

FIGURE 4. Frequency deviation of area-2 under Test Scenario 1.

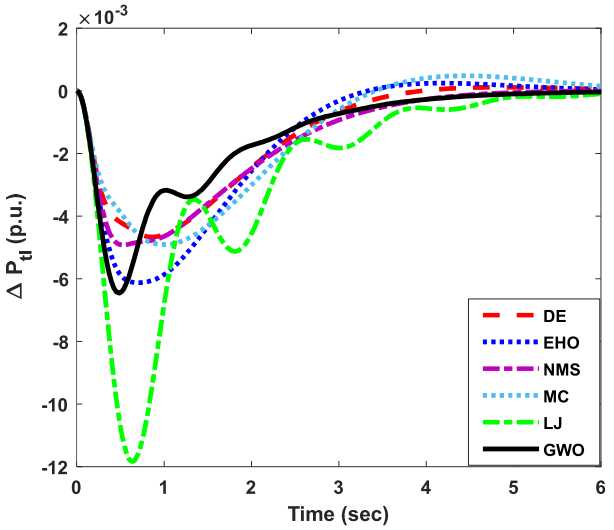

FIGURE 5. Deviation of tie-line power under Test Scenario 1.

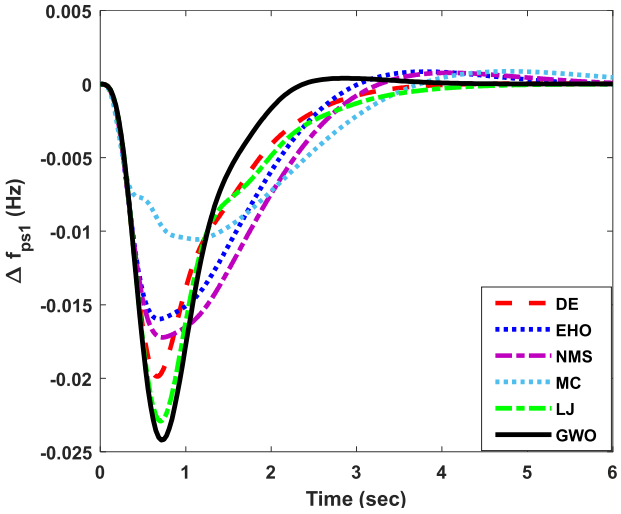

FIGURE 6. Frequency deviation of area-1 under Test Scenario 2.

where, $\overline{\Psi}$ represents position of prey in search space and $\overline{\Upsilon}$, $\overline{T}$ are coefficient vectors which are calculated as

$$\overline{\Upsilon} = 2\bar{\imath} \cdot \overline{\varphi}_1 - \bar{\imath} \tag{24}$$

$$\overline{T} = 2 \cdot \overline{\varphi}_2 \tag{25}$$

where, the component $\bar{\imath}$ declines linearly from 2 to 0 as the iterations increase, $\overline{\varphi}_1$ and $\overline{\varphi}_2$ are random vectors in range of [0, 1].

VI. RESULTS AND DISCUSSION

A two-area interconnected power system from Ali and Abd-Elazim [50] is examined in this research. In the MATLAB environment, all simulations are carried out. To convert a multi-objective illustration to a single-objective illustration, rank-sum-weight approach is employed. The Overall objective function is given in (16), whereas (9), (10), (11), and (12) depict the controller's boundary conditions. Appendix A and Appendix B contain all of the parameters for both the areas and controller, respectively. For time-domain simulations, six different test scenarios with a variety of load perturbations are taken into account. The following is a list of the six test scenarios considered:

- **Test Scenario 1:** At $t = 0$ s, a step load variation of $+0.05$ $p.u.$ is examined in area-1, with no load change in area-2.
- **Test Scenario 2:** At $t = 0$ s, a step load variation of $+0.05$ $p.u.$ is examined in area-2, with no load change in area-1.
- **Test Scenario 3:** At $t = 0$ s, a step load variation of $+0.05$ $p.u.$ is examined in both the areas.

TABLE 2. Test Scenario 1: Simulation results.

		DE	EHO	NMS	MC	LJ	GWO
Fitness	Γ	0.0329	0.0388	0.0328	0.0515	0.0605	**0.0276**
	Γ_1	0.0504	0.0601	0.0492	0.0805	0.0894	0.0407
	Γ_2	0.0128	0.0141	0.0140	0.0178	0.0242	0.0120
	Γ_3	0.0204	0.0240	0.0213	0.0320	0.0464	0.0191
Controller parameters	κ_{pg}	2.5322	1.7114	1.2271	2.8992	2.3422	2.1337
	κ_{ig}	2.9031	2.3584	2.3038	2.8007	2.7470	2.9228
	κ_{dg}	1.5492	0.9983	0.5518	1.3358	0.5120	0.6947
	η	220.32	196.31	282.08	177.02	168.41	227.80
Settling time (s)	Δf_{a1}	4.1047	4.0629	2.4990	4.9770	3.0945	2.2899
	Δf_{a2}	5.0789	4.8570	4.5371	6.0287	4.9459	4.5092
	ΔP_{tl}	5.4384	5.2660	4.6642	6.2377	4.8711	4.7510
Peak overshoots (p.u.)	Δf_{a1}	0.0296	0.0361	0.0334	0.0271	0.0604	0.0423
	Δf_{a2}	0.0116	0.0165	0.0137	0.0121	0.0355	0.0196
	ΔP_{tl}	0.0046	0.0061	0.0049	0.0049	0.0118	0.0064

TABLE 3. Test Scenario 2: Simulation results.

		DE	EHO	NMS	MC	LJ	GWO
Fitness	Γ	0.0270	0.0405	0.0470	0.0488	0.0302	**0.0267**
	Γ_1	0.0410	0.0631	0.0729	0.0757	0.0452	0.0414
	Γ_2	0.0112	0.0144	0.0171	0.0175	0.0130	0.0095
	Γ_3	0.0167	0.0251	0.0294	0.0305	0.0197	0.0168
Controller parameters	κ_{pg}	1.9163	2.2683	2.3421	2.8841	1.7625	2.7288
	κ_{ig}	2.6334	2.6896	2.4284	2.9357	2.3267	2.9572
	κ_{dg}	0.8045	0.7373	1.1834	0.7723	0.6614	0.9423
	η	193.37	449.94	294.20	164.11	332.45	495.21
Settling time (s)	Δf_{a1}	3.3203	4.9826	5.2206	6.6679	3.7129	2.2195
	Δf_{a2}	2.8192	4.1381	4.3575	5.3840	1.7048	3.0696
	ΔP_{tl}	3.4935	5.3383	5.6085	6.8540	3.8438	3.5978
Peak overshoots (p.u.)	Δf_{a1}	0.0198	0.0159	0.0172	0.0105	0.0229	0.0242
	Δf_{a2}	0.0414	0.0352	0.0365	0.0245	0.0451	0.0468
	ΔP_{tl}	0.0068	0.0060	0.0065	0.0043	0.0078	0.0083

TABLE 4. Test Scenario 3: Simulation results.

		DE	EHO	NMS	MC	LJ	GWO
Fitness	Γ	0.0512	0.0774	0.0471	0.1401	0.0640	**0.0313**
	Γ_1	0.0897	0.1356	0.0826	0.2455	0.1121	0.0548
	Γ_2	0	0	0	0	0	0
	Γ_3	0.0381	0.0576	0.0351	0.1043	0.0476	0.0233
Controller parameters	κ_{pg}	1.9583	1.7785	1.2738	2.1558	2.3989	1.7129
	κ_{ig}	2.7244	2.6724	2.4345	2.7358	2.5785	2.7014
	κ_{dg}	0.5351	0.3983	0.4260	0.7924	1.1329	0.6008
	η	434.92	458.87	303.41	146.04	254.10	442.12
Settling time (s)	Δf_{a1}	1.9951	3.9880	2.8601	5.8788	2.8715	2.1056
	Δf_{a2}	1.9951	3.9880	2.8601	5.8788	2.8715	2.1056
	ΔP_{tl}	0	0	0	0	0	0
Peak overshoots (p.u.)	Δf_{a1}	0.0649	0.0274	0.0368	0.0258	0.0692	0.0531
	Δf_{a2}	0.0649	0.0274	0.0368	0.0258	0.0692	0.0531
	ΔP_{tl}	0	0	0	0	0	0

- **Test Scenario 4:** At $t = 0$ *s*, a step load variation of $+0.050$ *p.u.* is considered in area-1, whereas at $t = 0$ *s*, a -0.05 *p.u.* step load variation is considered in area-2.
- **Test Scenario 5:** At $t = 0$ *s*, a step load variation of $+0.05$ *p.u.* is considered in area-1, whereas at $t = 0$ *s*, a $+0.10$ *p.u.* step load variation is considered in area-2.
- **Test Scenario 6:** At $t = 0$ *s*, a step load variation of $+0.10$ *p.u.* is considered in area-1, whereas at $t = 0$ *s*, a $+0.05$ *p.u.* step load variation is considered in area-2.

For various loading conditions as discussed in Test Scenario 1 to Test Scenario 6, the results are provided in Tables 2-7. In these tables, the performance of GWO-based PID controller is also compared with other controllers tuned using differential evolution (DE), elephant herding optimization (EHO), Nelder-Mead simplex (NMS), membrane computing (MC), and Luus-Jaakola (LJ) algorithms. The values of overall objective function, Γ, and three sub-objetives, Γ_1, Γ_2, and Γ_3, as provided in (16), are included in these findings. The controller parameters κ_{pg}, κ_{ig}, κ_{dg} and η for which the minimal value of the objective function is attained are also provided in these tables. These tables also indicate the settling times and peak overshoots of the variations in the frequencies and tie-line power.

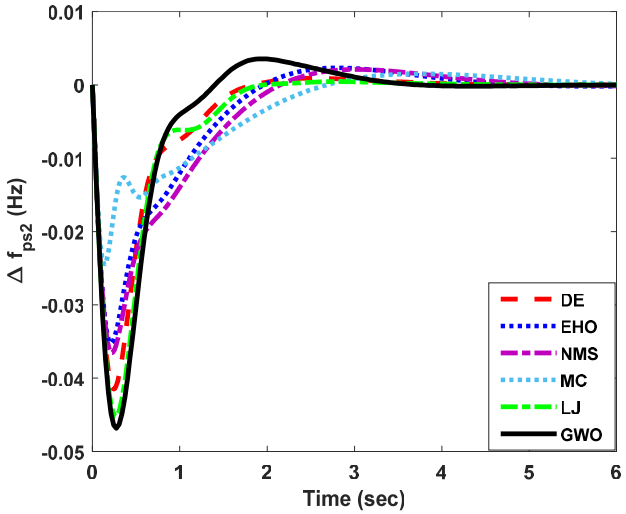

FIGURE 7. Frequency deviation of area-2 under Test Scenario 2.

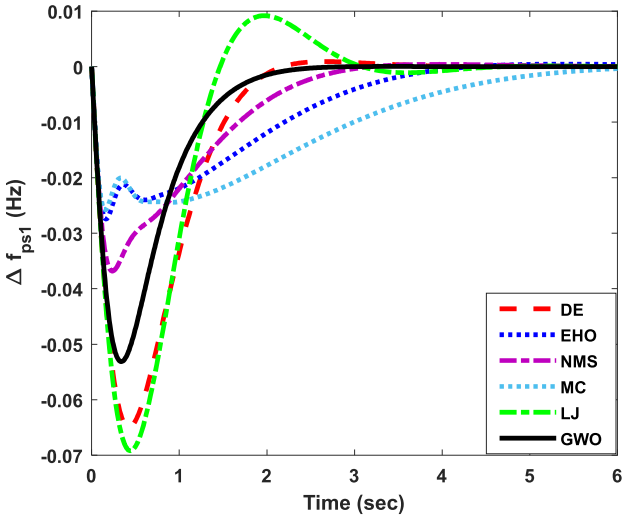

FIGURE 9. Frequency deviation of area-1 under Test Scenario 3.

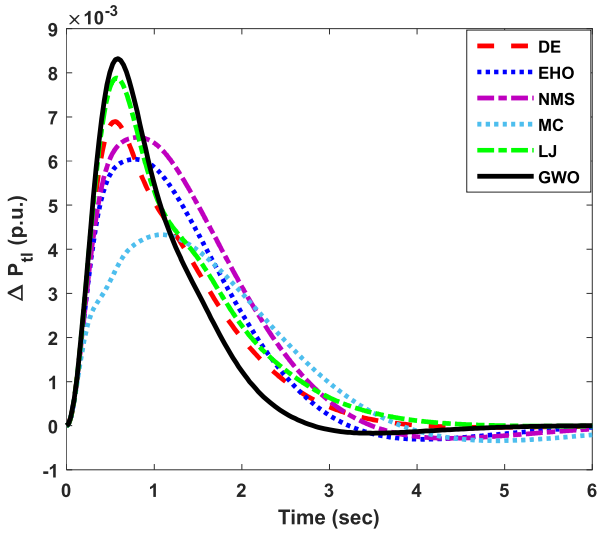

FIGURE 8. Deviation of tie-line power under Test Scenario 2.

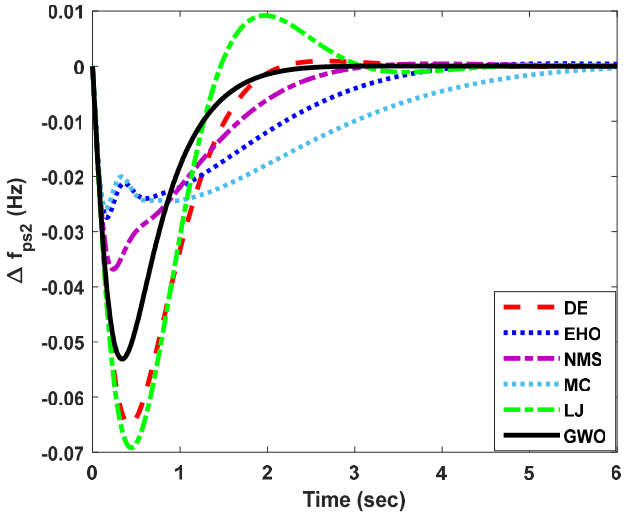

FIGURE 10. Frequency deviation of area-2 under Test Scenario 3.

For fair comparison of controllers designed using GWO, DE, EHO, NMS, MC, and LJ algorithms, a comparative study is also performed. For all six test circumstances stated above, every optimization algorithm is run consecutively 50 times. During simulations, a total 100 solutions are considered for each algorithm. The results for comparative study are provided in Table 8.

The simulation results for Test Scenario 1 are presented in Table 2. Fig.(s) 3, 4, and 5 demonstrate the deviations in frequencies of area-1, area-2, and change in tie-line power achieved respectively under this loading scenario. The GWO-based PID controller provides the smallest value of the objective function, Γ, when compared to other algorithm-based controllers. In addition, all three sub-objectives, Γ_1, Γ_2, and Γ_3 are determined to be minimal for the GWO-based PID controller. Further study of the simulation results reveals that the GWO-based PID controller achieves the shortest settling times for frequency fluctuations in area-1 and area-2.

Table 3 tabulates the simulation results for Test Scenario 2. Under the loading scenario described in Test Scenario 2, the suggested GWO-based PID controller achieves the lowest value of Γ. Along with the overall objective function being the least value, the sub-objective Γ_2 is determined to be the least. Fig.(s) 6, 7, and 8 illustrate the changes in frequencies of area-1, area-2, and tie-line power, respectively. Fig.(s) 6, 7, and 8 also indicate that the GWO-based PID controller outperforms the other five controllers.

Under the circumstances described in Test Scenario 3, variations in frequencies of area-1, area-2, and tie-line power obtained using the proposed GWO-based PID controller are shown in Fig.(s) 9, 10, and 11, respectively. Table 4 tabulates the simulation results for Test Scenario 3. The suggested GWO-based PID controller achieves the lowest value of Γ

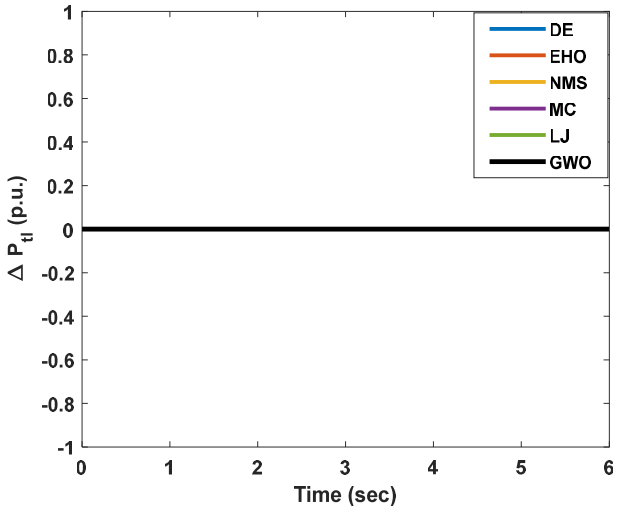

FIGURE 11. Deviation of tie-line power under Test Scenario 3.

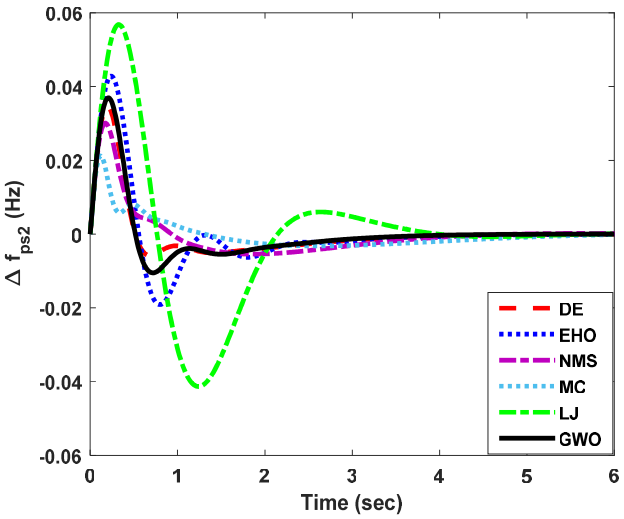

FIGURE 13. Frequency deviation of area-2 under Test Scenario 4.

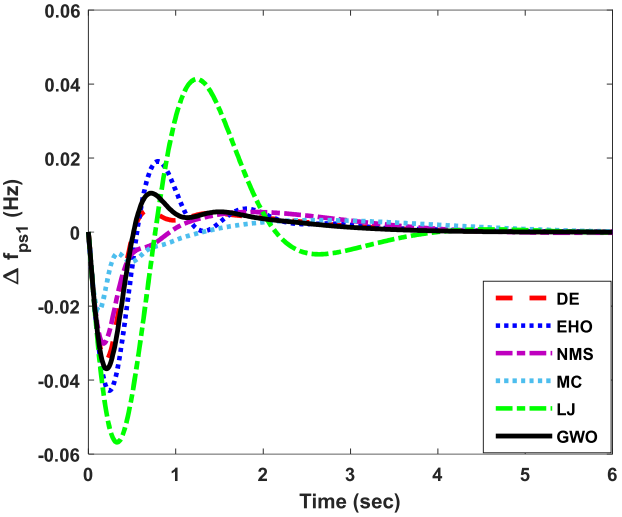

FIGURE 12. Frequency deviation of area-1 under Test Scenario 4.

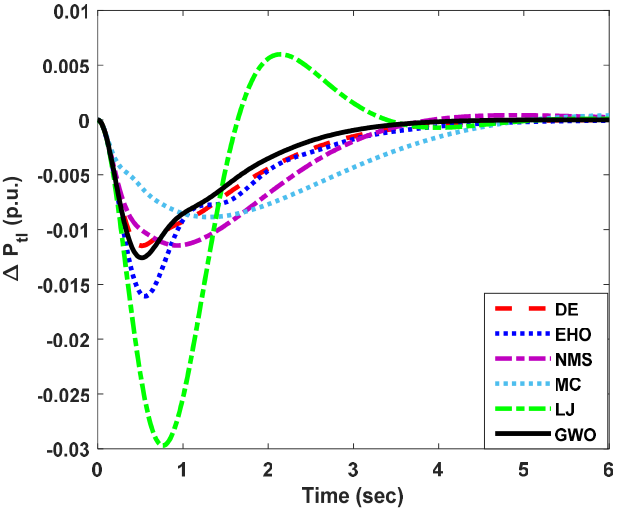

FIGURE 14. Deviation of tie-line power under Test Scenario 4.

as well as all sub-objectives, Γ_1, Γ_2, and Γ_3. As a result, the suggested GWO-based PID controller easily outperforms the other five controllers.

Similarly, the simulation results for Test Scenario 4 are presented in Table 5. The proposed GWO-based PID controller achieves the minimal values of the objective function, Γ, as well as all sub-objectives Γ_1, Γ_2, and Γ_3. Fig.(s) 12, 13, and 14 illustrate the deviations in frequencies of area-1, area-2, and tie-line power, respectively. The settling time of frequencies in area-1 and area-2, as well as the settling time of tie-line power are minimal in these plots. From the Test Scenario 4 findings, it is clear that the suggested GWO-based PID controller outperforms the other controllers investigated.

The deviations in frequencies of area-1, area-2, and tie-line power obtained using the proposed GWO-based PID controller for the loading condition described in Test Scenario 5 are shown in Fig.(s) 15, 16 and 17, respectively. Table 6 tabulates the simulation results for this Test Scenario 5. The suggested GWO-based PID controller produces the lowest values of the objective function, Γ, as well as all three sub-objective functions, Γ_1, Γ_2, and Γ_3. As a result, the proposed GWO-based PID controller is easily outperforming the existing controllers in Test Scenario 5.

The overall efficacy of the proposed GWO-based PID controller is evaluated using comparative statistical analysis. For each test scenario, the best, mean, worst, and standard deviation are calculated. The acquired values are listed in Table 8. It is evident from this table that the proposed GWO-based PID controller delivers the best value in all the scenarios. The DE-based controller is the next best option, followed by the MC-based controller. In the test scenarios, namely Test

TABLE 5. Test Scenario 4: Simulation results.

		DE	EHO	NMS	MC	LJ	GWO
Fitness	Γ	0.0367	0.0448	0.0521	0.0649	0.1011	**0.0327**
	Γ_1	0.0446	0.0559	0.0616	0.0666	0.1508	0.0426
	Γ_2	0.0253	0.0296	0.0359	0.0518	0.0388	0.0204
	Γ_3	0.0360	0.0421	0.0558	0.0862	0.0765	0.0275
Controller parameters	κ_{pg}	2.6611	1.6414	2.5869	2.7543	2.1658	2.8364
	κ_{ig}	2.8233	2.8136	2.4463	2.5614	2.0524	2.9243
	κ_{dg}	0.9305	0.5680	1.4420	1.7113	0.9637	1.0903
	η	424.02	137.13	279.43	395.31	204.18	408.96
Settling time (s)	Δf_{a1}	3.7902	3.6552	4.1817	5.5629	3.6615	3.4314
	Δf_{a2}	3.7902	3.6552	4.1817	5.5629	3.6615	3.4314
	ΔP_{tl}	4.3300	4.5086	6.1159	8.2727	4.2910	3.7793
Peak overshoots (p.u.)	Δf_{a1}	0.0347	0.0428	0.0301	0.0212	0.0568	0.0369
	Δf_{a2}	0.0347	0.0428	0.0301	0.0212	0.0568	0.0369
	ΔP_{tl}	0.0114	0.0160	0.0114	0.0088	0.0297	0.0125

TABLE 6. Test Scenario 5: Simulation results.

		DE	EHO	NMS	MC	LJ	GWO
Fitness	Γ	0.0686	0.0705	0.0624	0.0757	0.1187	**0.0517**
	Γ_1	0.1125	0.1164	0.1028	0.1254	0.1964	0.0852
	Γ_2	0.0116	0.0122	0.0105	0.0123	0.0186	0.0097
	Γ_3	0.0507	0.0492	0.0448	0.0533	0.0858	0.0348
Controller parameters	κ_{pg}	1.5917	2.1594	1.1101	2.9606	2.1332	1.7827
	κ_{ig}	2.7334	2.6138	2.3524	2.8451	2.9614	2.9022
	κ_{dg}	0.3881	0.8694	0.4044	0.8963	0.3748	0.4887
	η	497.94	196.35	220.03	191.99	400.57	184.96
Settling time (s)	Δf_{a1}	3.4898	3.3919	1.9310	4.3378	5.4689	2.5043
	Δf_{a2}	2.8336	2.5608	2.5483	3.3582	4.8412	1.6843
	ΔP_{tl}	4.2789	3.9172	2.5883	4.8007	6.2130	3.1865
Peak overshoots (p.u.)	Δf_{a1}	0.0752	0.0519	0.0841	0.0471	0.0749	0.0690
	Δf_{a2}	0.1159	0.0826	0.1214	0.0790	0.1169	0.1045
	ΔP_{tl}	0.0098	0.0063	0.0110	0.0056	0.0098	0.0088

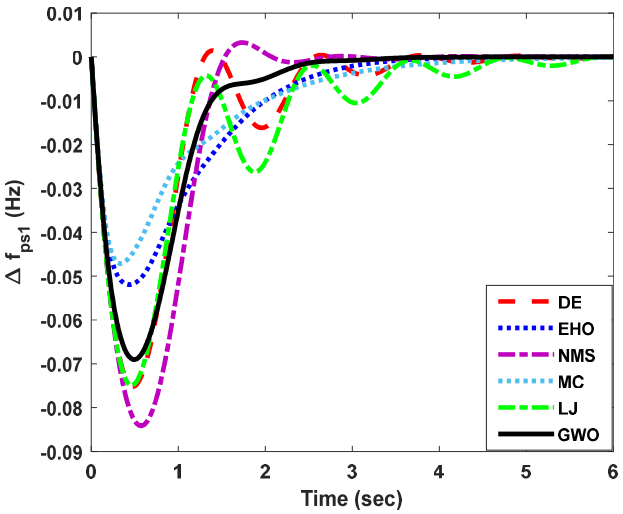

FIGURE 15. Frequency deviation of area-1 under Test Scenario 5.

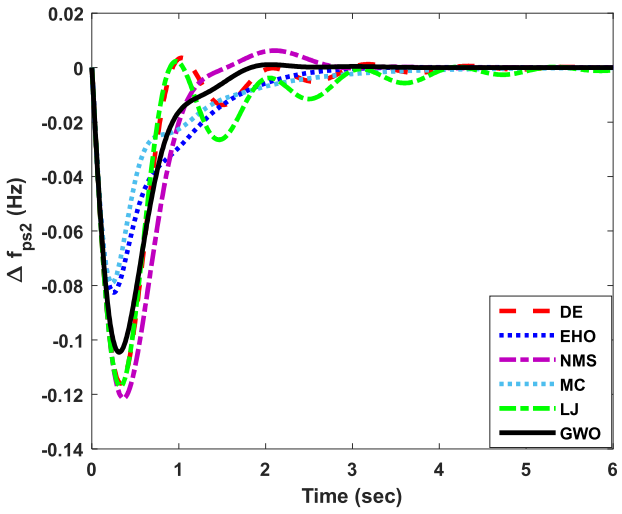

FIGURE 16. Frequency deviation of area-2 under Test Scenario 5.

Scenario 1, Test Scenario 2, Test Scenario 4, Test Scenario 5, and Test Scenario 6, the proposed GWO-based PID controller obtains the minimal mean value of objective function. In Test Scenario 1, Test Scenario 2, and Test Scenario 4, the proposed GWO-based PID controller has the lowest standard deviation values, whereas the DE-based controller have the least standard deviation values in Test Scenario 3 and Test Scenario 5 along with NMS-based controller having the least standard deviation value in Test Scenario 6. According to this statistical analysis, the suggested GWO-based PID controller is more effective than the other five controllers developed using the DE, EHO, NMS, MC, and LJ algorithms.

TABLE 7. Test Scenario 6: Simulation results.

		DE	EHO	NMS	MC	LJ	GWO
Fitness	Γ	0.1574	0.1554	0.0638	0.0759	0.1376	**0.0512**
	Γ_1	0.2600	0.2598	0.1058	0.1254	0.2305	0.0846
	Γ_2	0.0712	0.0216	0.0106	0.0129	0.0186	0.0085
	Γ_3	0.1107	0.1096	0.0442	0.0533	0.0970	0.0367
Controller parameters	κ_{pg}	2.0371	0.9565	1.9119	2.5847	0.9858	1.3186
	κ_{ig}	2.7657	2.5817	2.7808	2.8956	2.6851	2.7516
	κ_{dg}	0.6456	0.3716	0.8822	1.2152	0.4795	0.4536
	η	403.36	239.51	438.97	466.76	299.07	246.61
Settling time (s)	Δf_{a1}	2.7367	5.7320	2.9346	2.7219	4.6783	2.4523
	Δf_{a2}	3.1966	6.2006	2.5977	3.6371	5.0160	1.8939
	ΔP_{tl}	4.0572	6.7531	3.2403	4.1070	5.6262	2.4575
Peak overshoots (p.u.)	Δf_{a1}	0.1571	0.0613	0.0828	0.0875	0.0804	0.1139
	Δf_{a2}	0.1216	0.0440	0.0533	0.0555	0.0571	0.0768
	ΔP_{tl}	0.0163	0.0057	0.0065	0.0068	0.0069	0.0100

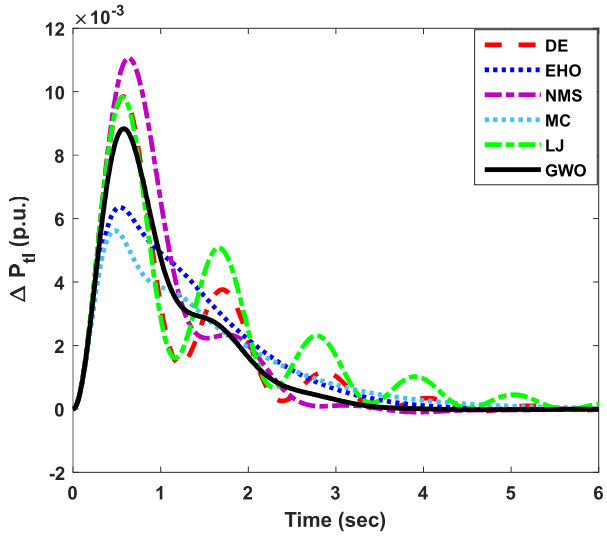

FIGURE 17. Deviation of tie-line power under Test Scenario 5.

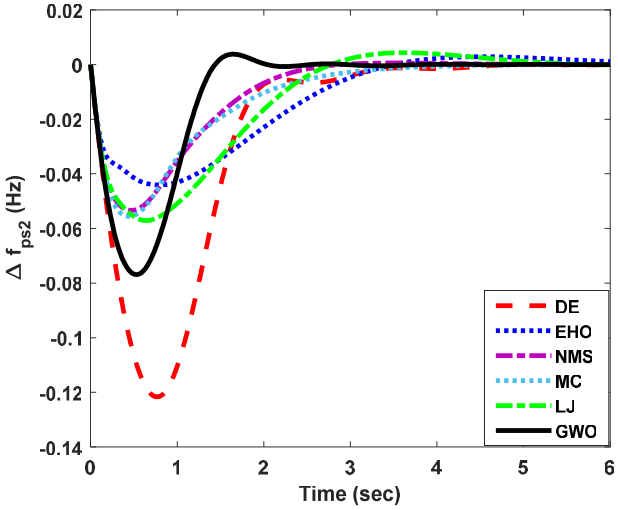

FIGURE 19. Frequency deviation of area-2 under Test Scenario 6.

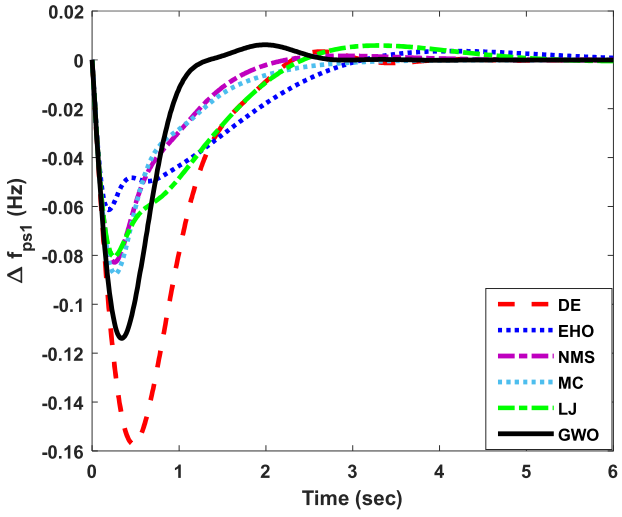

FIGURE 18. Frequency deviation of area-1 under Test Scenario 6.

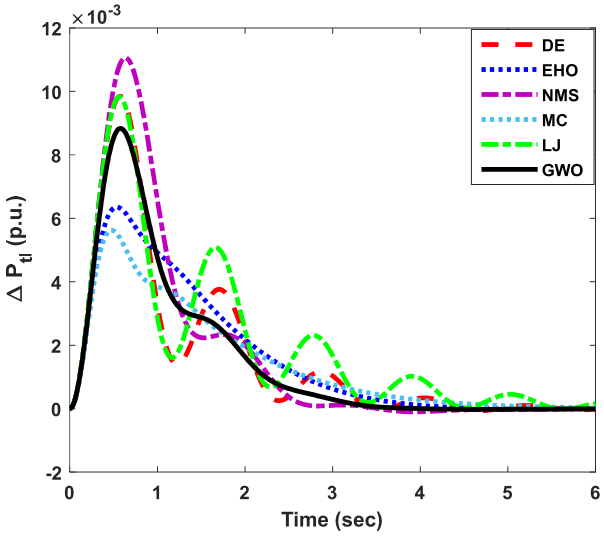

FIGURE 20. Deviation of tie-line power under Test Scenario 6.

Table 7 tabulates the simulation results obtained using the proposed GWO-based PID controller for the loading condition described in Test Scenario 6. The overall objective function, Γ, and all three sub-objectives, Γ_1, Γ_2,

TABLE 8. Statistical analysis.

Test Scenarios	Statistical measures	DE	EHO	NMS	MC	LJ	GWO
Test Scenario 1	Best	0.0329	0.0373	0.0310	0.0299	0.0274	**0.0219**
	Mean	0.0410	0.0470	0.0390	0.0441	0.0538	**0.0262**
	Worst	0.0528	0.0582	0.0613	0.0537	0.1074	**0.0291**
	Standard deviation	0.0072	0.0103	0.0126	0.0096	0.0326	**0.0026**
Test Scenario 2	Best	0.0270	0.0255	0.0353	0.0255	0.0302	**0.0242**
	Mean	0.0382	0.0448	0.0413	0.0401	0.0737	**0.0281**
	Worst	0.0636	0.0694	0.0470	0.0634	0.1938	**0.0328**
	Standard deviation	0.0147	0.0193	0.0054	0.0159	0.0682	**0.0036**
Test Scenario 3	Best	0.0347	0.0331	0.0315	0.0379	0.0501	**0.0313**
	Mean	**0.0415**	0.0739	0.0487	0.0635	0.0726	0.0666
	Worst	**0.0512**	0.1582	0.0813	0.1401	0.1038	0.1052
	Standard deviation	**0.0075**	0.0501	0.0195	0.0430	0.0229	0.0267
Test Scenario 4	Best	0.0341	0.0352	0.0422	0.0422	0.0496	**0.0326**
	Mean	0.0454	0.0411	0.0467	0.0689	0.0725	**0.0343**
	Worst	0.0643	0.0448	0.0521	0.0945	0.1011	**0.0386**
	Standard deviation	0.0123	0.0036	0.0035	0.0194	0.0260	**0.0025**
Test Scenario 5	Best	0.0541	0.0687	0.0624	0.0757	0.0678	**0.0447**
	Mean	0.0675	0.0806	0.1040	0.1018	0.1170	**0.0564**
	Worst	**0.0750**	0.1010	0.1744	0.1382	0.1868	0.0831
	Standard deviation	**0.0086**	0.0149	0.0511	0.0253	0.0470	0.0152
Test Scenario 6	Best	0.0557	0.0821	0.0638	0.0682	0.0853	**0.0512**
	Mean	**0.0835**	0.1061	0.0861	0.1019	0.1328	0.1127
	Worst	0.1574	0.1554	**0.1097**	0.1393	0.2001	0.2088
	Standard deviation	0.0423	0.0284	**0.0182**	0.0312	0.0469	0.0658

and Γ_3, have the minimal values. The frequency deviations of area-1, area-2, and tie-line power obtained using the proposed GWO-based PID controller are shown in Fig.(s) 18, 19, and 20, respectively. As can be seen in the plots, the suggested GWO-based PID controller clearly achieves the shortest settling time for frequency variations in area-1, area-2, and power deviations in tie-line. As a result, it is evident that the suggested GWO-based PID controller outperforms the other five controllers in this test instance also.

VII. CONCLUSION

For tackling the problem of AGC, GWO assisted rank-sum-weight method based controller is proposed in this article. The controller design takes into account three objectives. These separate objectives result in a multi-objective formulation. This multi-objective formulation is converted into single objective formulation using a decision making tool, rank-sum-weight method. The suggested GWO assisted rank-sum-weight method based controller is compared to controllers tuned using differential evolution (DE), elephant herding optimization (EHO), Nelder-Mead simplex (NMS), membrane computing (MC), and Luus-Jaakola (LJ) algorithms for ensuring the effectiveness. The effectiveness of suggested GWO assisted rank-sum-weight method based controller is tested for six distinct scenarios involving a variety of perturbations in the range of mild load variations to large load variations in interconnected areas. The numerical results demonstrate the superiority and efficacy of the suggested GWO-based PID controller in comparison with other optimization based controllers. The improved nature of the suggested controller for an AGC issue is demonstrated by time-domain simulations for variations in the frequencies of the regions under various scenarios. A comparative statistical analysis is performed for all the scenarios to assess the overall effectiveness of the suggested GWO-based PID controller.

The examination of AGC issue with non-linear models and implementation of renewable energies is the future topic of this research. The efficacy of rank-sum-weight method should also be investigated for other multi-objective formulations in the area of AGC. Moreover, other optimization algorithms [52], [53] should also be investigated for single-objective and multi-objective formulations [54], [55] of AGC problem.

DATA AVAILABILITY

My manuscript has no associated data.

APPENDIX A

PARAMETERS OF TWO-AREA INTERCONNECTED POWER SYSTEM

System frequency	$f = 60$ Hz;
Frequency bias factors	$\beta_{a1}, \beta_{a2} = 0.05$ p.u. Mw/Hz;
Governor speed regulation constants	$R_{a1}, R_{a2} = 2.4$ Hz/p.u.;
Governor time constants	$\tau_{gr1}, \tau_{gr2} = 0.08$ s;
Turbine time constants	$\tau_{te1}, \tau_{te2} = 0.3$ s;
Power system gains	$\kappa_{a1}, \kappa_{a2} = 120$ Hz/p.u. Mw;
Power system time constants	$\tau_{a1}, \tau_{a2} = 20$ s;
Synchronizing torque co-efficient	$\tau_{12} = 0.545$ p.u.;
Ratio of rated power at area-1 to area-2	$a_{12} = -1$.

APPENDIX B

BOUNDARY CONDITIONS OF CONTROLLER

Proportional gain	$\kappa_{pg}^{min} = 0; \kappa_{pg}^{max} = 3;$
Integral gain	$\kappa_{ig}^{min} = 0; \kappa_{ig}^{max} = 3;$
Derivative gain	$\kappa_{dg}^{min} = 0; \kappa_{dg}^{max} = 3;$
Filter gain	$n^{min} = 0; n^{max} = 500.$

REFERENCES

[1] A. Kumar and O. Singh, "Optimal automatic generation control in multi-area power systems with diverse energy sources," in *Advances in Energy Technology*. Cham, Switzerland: Springer, 2022, pp. 289–300.

[2] D. Tripathy, A. K. Barik, N. B. D. Choudhury, and B. K. Sahu, "Performance comparison of SMO-based fuzzy PID controller for load frequency control," in *Soft Computing for Problem Solving*. Cham, Switzerland: Springer, 2019, pp. 879–892.

[3] D. Boopathi, K. Jagatheesan, B. Anand, V. Kumarakrishnan, and S. Samanta, "Effect of sustainable energy sources for load frequency control (LFC) of single-area wind power systems," in *Industrial Transformation*. Boca Raton, FL, USA: CRC Press, 2022, pp. 87–98.

[4] T. Muthukumar, K. Jagatheesan, and S. Samanta, "Mayfly algorithm-based PID controller for LFC of multi-sources single area power system," in *Intelligence Enabled Research*. Cham, Switzerland: Springer, 2022, pp. 53–64.

[5] V. Kumarakrishnan, G. Vijayakumar, K. Jagatheesan, D. Boopathi, B. Anand, and V. K. Naidu, "PSO optimum design-PID controller for frequency management of single area multi-source power generating system," in *Contemporary Issues in Communication, Cloud and Big Data Analytics*. Cham, Switzerland: Springer, 2022, pp. 373–383.

[6] A. Daraz, S. Abdullah, H. Mokhlis, I. U. Haq, G. Fareed, and N. N. Mansor, "Fitness dependent optimizer-based automatic generation control of multi-source interconnected power system with non-linearities," *IEEE Access*, vol. 8, pp. 100989–101003, 2020.

[7] A. Daraz, S. A. Malik, H. Mokhlis, I. U. Haq, F. Zafar, and N. N. Mansor, "Improved-fitness dependent optimizer based FOI-PD controller for automatic generation control of multi-source interconnected power system in deregulated environment," *IEEE Access*, vol. 8, pp. 197757–197775, 2020.

[8] L. Xi, L. Zhang, Y. Xu, S. Wang, and C. Yang, "Automatic generation control based on multiple-step greedy attribute and multiple-level allocation strategy," *CSEE J. Power Energy Syst.*, vol. 8, no. 1, pp. 281–292, 2022.

[9] R. Patel, L. Meegahapola, L. Wang, X. Yu, and B. McGrath, "Automatic generation control of multi-area power system with network constraints and communication delays," *J. Modern Power Syst. Clean Energy*, vol. 8, no. 3, pp. 454–463, 2020.

[10] S. Chatterjee and A. N. Mohammed, "Performance evaluation of novel moth flame optimization (MFO) technique for AGC of hydro system," in *IoT With Smart Systems*. Cham, Switzerland: Springer, 2022, pp. 377–392.

[11] Y. Arya, P. Dahiya, E. Çelik, G. Sharma, H. Gözde, and I. Nasiruddin, "AGC performance amelioration in multi-area interconnected thermal and thermal-hydro-gas power systems using a novel controller," *Eng. Sci. Technol., Int. J.*, vol. 24, no. 2, pp. 384–396, Apr. 2021.

[12] K. Jagatheesan, B. Anand, S. Samanta, N. Dey, A. S. Ashour, and V. E. Balas, "Design of a proportional-integral-derivative controller for an automatic generation control of multi-area power thermal systems using firefly algorithm," *IEEE/CAA J. Autom. Sinica*, vol. 6, no. 2, pp. 503–515, Mar. 2019.

[13] C. Tan, Y. Li, Q. Lan, X. Xiao, Q. Ding, X. Zhang, M. Wang, X. Teng, and Y. Wang, "Multi-area automatic generation control scheme considering frequency quality in Southwest China grid: Challenges and solutions," *IEEE Access*, vol. 8, pp. 199813–199828, 2020.

[14] R. Patel, C. Li, L. Meegahapola, B. McGrath, and X. Yu, "Enhancing optimal automatic generation control in a multi-area power system with diverse energy resources," *IEEE Trans. Power Syst.*, vol. 34, no. 5, pp. 3465–3475, Sep. 2019.

[15] S. Patel, B. Mohanty, and K. S. Simhadri, "Frequency stability analysis of power system using competition over resources technique optimized PIDA controller," *Iranian J. Sci. Technol., Trans. Electr. Eng.*, vol. 46, no. 1, pp. 57–75, Mar. 2022.

[16] S.-E.-I. Hasseni, L. Abdou, and H.-E. Glida, "Parameters tuning of a quadrotor PID controllers by using nature-inspired algorithms," *Evol. Intell.*, vol. 14, no. 1, pp. 61–73, Mar. 2021.

[17] R. Kumar Khadanga, A. Kumar, and S. Panda, "Frequency control in hybrid distributed power systems via type-2 fuzzy PID controller," *IET Renew. Power Gener.*, vol. 15, no. 8, pp. 1706–1723, Jun. 2021.

[18] T. Prakash and V. P. Singh, "A novel membrane computing inspired Jaya algorithm based automatic generation control of multi-area interconnected power system," in *Hybrid Metaheuristics: Research and Applications*, vol. 84. 2018, p. 89, doi: 0.1142/9789813270237_0004.

[19] S. P. Singh, T. Prakash, V. P. Singh, and M. G. Babu, "Analytic hierarchy process based automatic generation control of multi-area interconnected power system using Jaya algorithm," *Eng. Appl. Artif. Intell.*, vol. 60, pp. 35–44, Apr. 2017.

[20] S. M. Ghamari, H. G. Narm, and H. Mollaee, "Fractional-order fuzzy PID controller design on buck converter with antlion optimization algorithm," *IET Control Theory Appl.*, vol. 16, no. 3, pp. 340–352, Feb. 2022.

[21] G. Fusco and M. Russo, "Tuning of multivariable PI robust controllers for the decentralized voltage regulation in grid-connected distribution networks with distributed generation," *Int. J. Dyn. Control*, vol. 8, no. 1, pp. 278–290, Mar. 2020.

[22] S. Priyadarshani, K. R. Subhashini, and J. K. Satapathy, "Pathfinder algorithm optimized fractional order tilt-integral-derivative (FOTID) controller for automatic generation control of multi-source power system," *Microsyst. Technol.*, vol. 27, no. 1, pp. 23–35, 2020.

[23] B. Mohanty, "Performance analysis of moth flame optimization algorithm for AGC system," *Int. J. Model. Simul.*, vol. 39, no. 2, pp. 73–87, Apr. 2019.

[24] J. M. R. Chintu, R. K. Sahu, and S. Panda, "Adaptive differential evolution tuned hybrid fuzzy PD-PI controller for automatic generation control of power systems," *Int. J. Ambient Energy*, vol. 43, no. 1, pp. 1–16, 2019.

[25] S. Padhy and S. Panda, "A hybrid stochastic fractal search and pattern search technique based cascade PI-PD controller for automatic generation control of multi-source power systems in presence of plug in electric vehicles," *CAAI Trans. Intell. Technol.*, vol. 2, no. 1, pp. 12–25, 2017.

[26] A. Behera, T. K. Panigrahi, P. K. Ray, and A. K. Sahoo, "A novel cascaded PID controller for automatic generation control analysis with renewable sources," *IEEE/CAA J. Autom. Sinica*, vol. 6, no. 6, pp. 1438–1451, Nov. 2019.

[27] R. Singh and I. Sen, "Tuning of PID controller based AGC system using genetic algorithms," in *Proc. IEEE Region Conf. TENCON*, vol. 100, 2004, pp. 531–534.

[28] Y. L. Abdel-Magid and M. M. Dawoud, "Optimal AGC tuning with genetic algorithms," *Electr. Power Syst. Res.*, vol. 38, no. 3, pp. 231–238, Sep. 1996.

[29] P. Mohanty, R. K. Sahu, and S. Panda, "A novel hybrid many optimizing liaisons gravitational search algorithm approach for AGC of power systems," *Automatika*, vol. 61, no. 1, pp. 158–178, Jan. 2020.

[30] R. K. Sahu, S. Panda, and S. Padhan, "Optimal gravitational search algorithm for automatic generation control of interconnected power systems," *Ain Shams Eng. J.*, vol. 5, no. 3, pp. 721–733, Sep. 2014.

[31] J. Nanda, S. Mishra, and L. C. Saikia, "Maiden application of bacterial foraging-based optimization technique in multiarea automatic generation control," *IEEE Trans. Power Syst.*, vol. 24, no. 2, pp. 602–609, May 2009.

[32] I. Nasiruddin, T. S. Bhatti, and N. Hakimuddin, "Automatic generation control in an interconnected power system incorporating diverse source power plants using bacteria foraging optimization technique," *Electr. Power Compon. Syst.*, vol. 43, no. 2, pp. 189–199, Jan. 2015.

[33] S. S. Pati, A. Behera, and T. K. Panigrahi, "Automatic generation control of multi-area system incorporating renewable unit and energy storage by bat algorithm," in *Innovative Product Design and Intelligent Manufacturing Systems*. Cham, Switzerland: Springer, 2020, pp. 713–722.

[34] S. M. Abd-Elazim and E. S. Ali, "Load frequency controller design via BAT algorithm for nonlinear interconnected power system," *Int. J. Electr. Power Energy Syst.*, vol. 77, pp. 166–177, May 2016.

[35] A. Rai and D. K. Das, "An adaptive class topper optimization algorithm-based automatic generation control of multi-area interconnected power system with nonlinearity," *Trans. Indian Nat. Acad. Eng.*, vol. 7, no. 1, pp. 1–15, 2022.

[36] R. K. Sahu, T. S. Gorripotu, and S. Panda, "Automatic generation control of multi-area power systems with diverse energy sources using teaching learning based optimization algorithm," *Eng. Sci. Technol., Int. J.*, vol. 19, no. 1, pp. 113–134, 2016.

[37] P. C. Pradhan, R. K. Sahu, and S. Panda, "Firefly algorithm optimized fuzzy PID controller for AGC of multi-area multi-source power systems with UPFC and SMES," *Eng. Sci. Technol., Int. J.*, vol. 19, no. 1, pp. 338–354, Mar. 2016.

[38] T. S. Gorripotu, R. K. Sahu, and S. Panda, "Application of firefly algorithm for AGC under deregulated power system," in *Computational Intelligence in Data Mining*, vol. 1. Cham, Switzerland: Springer, 2015, pp. 677–687.

[39] N. Pathak, T. S. Bhatti, A. Verma, and I. Nasiruddin, "AGC of two area power system based on different power output control strategies of thermal power generation," *IEEE Trans. Power Syst.*, vol. 33, no. 2, pp. 2040–2052, Mar. 2017.

[40] J. Seekuka, R. Rattanawaorahirunkul, S. Sansri, S. Sangsuriyan, and A. Prakonsant, "AGC using particle swarm optimization based PID controller design for two area power system," in *Proc. Int. Comput. Sci. Eng. Conf. (ICSEC)*, Dec. 2016, pp. 1–4.
[41] V. Kumarakrishnan, G. Vijayakumar, D. Boopathi, K. Jagatheesan, S. Saravanan, and B. Anand, "Frequency regulation of interconnected power generating system using ant colony optimization technique tuned PID controller," in *Control and Measurement Applications for Smart Grid*. Cham, Switzerland: Springer, 2022, pp. 129–141.
[42] K. Naidu, H. Mokhlis, A. H. A. Bakar, and V. Terzija, "Performance investigation of ABC algorithm in multi-area power system with multiple interconnected generators," *Appl. Soft Comput.*, vol. 57, pp. 436–451, Aug. 2017.
[43] S. Bhongade, "Automatic generation control of two-area ST-Thermal power system using Jaya algorithm," *Int. J. Smart Grid-ijSmartGrid*, vol. 2, no. 2, pp. 99–110, 2018.
[44] M. H. Hany, "Whale optimisation algorithm for automatic generation control of interconnected modern power systems including renewable energy sources," *IET Gener. Transm. Distrib.*, vol. 12, no. 3, pp. 607–614, Feb. 2018.
[45] K. Ullah, A. Basit, Z. Ullah, S. Aslam, and H. Herodotou, "Automatic generation control strategies in conventional and modern power systems: A comprehensive overview," *Energies*, vol. 14, no. 9, p. 2376, Apr. 2021.
[46] R. K. Sahu, S. Panda, and G. T. C. Sekhar, "A novel hybrid PSO-PS optimized fuzzy PI controller for AGC in multi area interconnected power systems," *Int. J. Electr. Power Energy Syst.*, vol. 64, pp. 880–893, Jan. 2015.
[47] N. Jaleeli, L. S. VanSlyck, D. N. Ewart, L. H. Fink, and A. G. Hoffmann, "Understanding automatic generation control," *IEEE Trans. Power Syst.*, vol. 7, no. 3, pp. 1106–1122, Aug. 1992.
[48] C. N. S. Kalyan and G. S. Rao, "Coordinated control strategy for simultaneous frequency and voltage stabilisation of the multi-area interconnected system considering communication time delays," *Int. J. Ambient Energy*, pp. 1–13, Aug. 2021, doi: 10./01430750.2021.1967192.
[49] W. G. Stillwell, D. A. Seaver, and W. Edwards, "A comparison of weight approximation techniques in multiattribute utility decision making," *Organizational Behav. Hum. Perform.*, vol. 28, no. 1, pp. 62–77, Aug. 1981.
[50] E. S. Ali and S. M. Abd-Elazim, "Bacteria foraging optimization algorithm based load frequency controller for interconnected power system," *Int. J. Electr. Power Energy Syst.*, vol. 33, no. 3, pp. 633–638, Mar. 2011.
[51] S. Mirjalili, S. M. Mirjalili, and A. Lewis, "Grey wolf optimizer," *Adv. Eng. Softw.*, vol. 69, pp. 46–61, Mar. 2014.
[52] P. Liu, Q. Hu, K. Jin, G. Yu, and Z. Tang, "Toward the energy-saving optimization of WLAN deployment in real 3-D environment: A hybrid swarm intelligent method," *IEEE Syst. J.*, vol. 16, no. 2, pp. 2425–2436, Jun. 2022.
[53] J. Fan, Q. Hu, and Z. Tang, "Predicting vacant parking space availability: An SVR method with fruit fly optimisation," *IET Intell. Transp. Syst.*, vol. 12, no. 10, pp. 1414–1420, Dec. 2018.
[54] N. Yang, Z. Tang, X. Cai, L. Chen, and Q. Hu, "Cooperative multi-population Harris hawks optimization for many-objective optimization," *Complex Intell. Syst.*, pp. 1–34, Feb. 2022, doi: 10.1007/s40747-022-00670.
[55] K. Jin, X. Cai, J. Du, H. Park, and Z. Tang, "Toward energy efficient and balanced user associations and power allocations in multi-connectivity enabled mmWave networks," *IEEE Trans. Green Commun. Netw.*, early access, May 3, 2022, doi: 10.1109/TGCN.2022.3172355.

P. J. KRISHNA (Member, IEEE) was born in Visakhapatnam, Andhra Pradesh, India, in July 1998. He received the Diploma degree in electrical and electronics engineering from Government Polytechnic, Visakhapatnam, in 2017, and the B.Tech. degree in electrical and electronics engineering from the Anil Neerukonda Institute of Technology and Sciences, Sangivalasa, Andhra Pradesh, in 2020. He is currently pursuing the M.Tech. degree in power systems engineering with the Malaviya National Institute of Technology Jaipur, Jaipur, India. His research interests include power system modeling, optimization, and control systems.

V. P. MEENA (Member, IEEE) was born in Karauli, Rajasthan, India, in April 1996. He received the B.Tech. degree in electrical engineering from the Government Engineering College, Bikaner, India, in 2018, and the M.Tech. degree in power system engineering from the Indian Institute of Technology Roorkee (IIT Roorkee), in July 2020. He is currently pursuing the Ph.D. degree in electrical engineering with the Malaviya National Institute of Technology (MNIT) Jaipur, Jaipur, India. The focus of his Ph.D. research is on approximation and controller design for continuous and discrete interval systems. He contributed to the body of knowledge by publishing several research papers in international journals and conferences. His research interests include system modeling, controller design for desalination systems, interval systems, model order reduction, applications of optimization algorithms power systems, power electronics, and artificial intelligence.

V. P. SINGH (Senior Member, IEEE) received the B.Tech. degree (Hons.) in electrical engineering from Uttar Pradesh Technical University, Lucknow, India, in 2007, and the M.Tech. degree in control and instrumentation and the Ph.D. degree in electrical engineering from the Motilal Nehru National Institute of Technology, Allahabad, India, in 2009 and 2013, respectively. He worked as an Assistant Professor with the National Institute of Technology Raipur, India. He is currently working as an Assistant Professor at the Malaviya National Institute of Technology Jaipur, Jaipur, India. His research interests include system modeling, model order reduction, and applications of optimization. He has several conferences and journal publications to his credit.

BASEEM KHAN (Senior Member, IEEE) received the B.Eng. degree in electrical engineering from Rajiv Gandhi Technological University, Bhopal, India, in 2008, and the M.Tech. and D.Phil. degrees in electrical engineering from the Maulana Azad National Institute of Technology, Bhopal, in 2010 and 2014, respectively. He is currently working as a Faculty Member with Hawassa University, Ethiopia. He has published more than 100 research articles in well reputable research journals, including the IEEE Transactions, IEEE Access, *Computers and Electrical Engineering* (Elsevier), *IET GTD*, *IET RPG*, and *IET Power Electronics*. Further, he has published authored and edited books with Wiley, CRC Press, and Elsevier. His research interests include power system restructuring, power system planning, smart grid technologies, meta-heuristic optimization techniques, reliability analysis of renewable energy systems, power quality analysis, and renewable energy integration.